A&A manuscript no.
(will be inserted by hand later)

Your thesaurus codes are:
02(02.13.1; 02.09.1; 11.13.2; 11.19.2; 11.09.4; 09.11.1)

ASTRONOMY
AND
ASTROPHYSICS
1.2.2008

arXiv:astro-ph/9610167v2 23 Nov 1997

The galactic dynamo effect due to Parker-shearing instability of magnetic flux tubes

I. General formalism and the linear approximation.

M. Hanasz[1] **and H. Lesch**[2]

[1] Institute of Astronomy, Nicolaus Copernicus University, ul. Chopina 12/18, PL-87-100 Torun, Poland.
[2] University Observatory, München University, Scheinerstr. 1, 81679 München , Germany

Received July 31, 1996/ accepted October 30, 1996

Abstract. In this paper we investigate the idea of Hanasz & Lesch 1993 that the galactic dynamo effect is due to the Parker instability of magnetic flux tubes. In addition to the former approach, we take into account more general physical conditions in this paper, by incorporating cosmic rays and differential forces due to the axisymmetric differential rotation and the density waves as well.

We present the theory of slender magnetic flux tube dynamics in the thin flux tube approximation and the Lagrange description. This is the application of the formalism obtained for solar magnetic flux tubes by Spruit (1981), to the galactic conditions. We perform a linear stability analysis for the Parker-shearing instability of magnetic flux tubes in galactic discs and then calculate the dynamo coefficients.

We present a number of new effects which are very essential for cosmological and contemporary evolution of galactic magnetic fields. First of all we demonstrate that a very strong dynamo α-effect is possible in the limit of weak magnetic fields in presence of cosmic rays. Second, we show that the differential force resulting from axisymmetric differential rotation and the linear density waves causes that the α-effect is essentially magnified in galactic arms and switched off in the interarm regions. Moreover, we predict a non-uniform magnetic field in spiral arms and well aligned one in interarm regions. These properties are well confirmed by recent observational results by Beck & Hoernes (1996)

Key words: Magnetic fields – Instabilities – Galaxies: magnetic fields – spiral – ISM: kinematics and dynamics of

1. Introduction

The origin of galactic magnetic fields is a long standing problem in theoretical astrophysics. Virtually all spiral galaxies have magnetic fields of a few μG which are spatially coherent over several parsecs (see Kronberg 1994; Beck et al. 1996 for recent reviews). This implies that the average magnetic energy density is comparable to the average energy densities of cosmic rays and the interstellar medium, which in turn suggests that galactic magnetic fields reached a state of saturation some unknown time in the past. In face of the Faraday rotation measurements of Wolfe et al. (1992), which indicate μG fields in damped Lymanα clouds at redshifts of 2 (the universe was about 1-2 Gigayears old), the saturation has to be very rapid. Since galaxies are so large (and damped Lymanα clouds are supposed to be progenitors of disc galaxies), and their constituent gases are highly conducting, the dissipative time scale for these fields is considerably longer than a Hubble time. Either the magnetic fields are simply the result of some pre-existing cosmological field (Kulsrud 1990) or they are spectacular examples of fast dynamos, in which rapid magnetic reconnection takes over the role of the traditional eddy diffusivity (Parker 1992)

Nowadays the regular magnetic fields in the discs of spiral galaxies are usually considered to be the result of large-scale dynamo action, involving a collective induction effect of turbulence (α-effect) and differential rotation. Both mechanisms have been described in detail in a huge number of articles (e.g. Kronberg 1994; Beck et al. 1996 and references therein). A small seed field is exponentially amplified by the interplay of turbulent motions perpendicular to the disc generating a radial magnetic field component $B_{\rm r}$ from an azimuthal component B_φ. Differential rotation in the galactic disc then closes the loop by generating B_φ from $B_{\rm r}$. The magnetic field grows exponentially on time scales of the order of a Gigayear (Camenzind

---

Send offprint requests to: M. Hanasz, e-mail: *mhanasz@astri.uni.torun.pl*

and Lesch 1994). The growth time raises the problem of magnetic field amplification at high redshifts. The typical seed field strengths is of the order of 10^{-18} G and the typical present magnetic field strength is of the order of 10^{-6} G. The e-folding times of the dynamo magnification process have to be of the order of a few hundreds of Myr or even a few tens of Myr for the total time of growth 10 Gyr or 1 Gyr respectively. Such a short e-folding time seems to be unavailable within the classical dynamo models (Lesch and Chiba 1995).

Whereas the differential rotation of galactic disc is a clearly observed feature of spiral galaxies, there is no general agreement on the source or value of α. The helicity α is connected with the interstellar turbulence, which may be fed by several sources (warm gas, hot bubbles, cold filaments, supernova explosions, cloud-cloud collisions, OB-associations, the galactic fountain, etc...). These violent motions agitate the interstellar gases and drive turbulence. The classical α-effect measures the field-aligned electromotive force resulting from magnetic field lines twisted by the turbulence. Originally the dynamics of these field lines is governed by external turbulent motions like supernova explosions (Ruzmaikin, Sokoloff and Shukurov 1988; Ferriere 1993). However, attempts to compute the several components of the helicity tensor α_{ij} resulting from exploding supernovas or superbubbles resulted in values considerably to small to allow for fast and efficient dynamo action (Kaisig et al. 1993). Nevertheless, the most recent calculation of the superbubble contribution to the helicity tensor by Ferriere (1996) makes the superbubble model more attractive. Beside that time scale problem, the recent observations by Beck and Hoernes (1996) raise the question what kind of global process in a galactic disc can explain the "magnetic arms" in NGC 6946. They report the detection of two highly polarized magnetic features which are 0.5 - 1 kpc wide and about 12 kpc long and have greater symmetry than the optical arms. These features cannot be explained by standard dynamo models.

The usual dynamo models treat the magnetic field as a superposition of a homogeneous mean field and a fluctuating, turbulent field component, which is responsible for the turbulent diffusion and the helicity, as well. We considered in a first paper (Hanasz and Lesch 1993, hereafter HL'93) the Parker instability of magnetic flux tubes (Parker 1955, 1966, 1967a,b) as the source for the helicity, taking into account the observed complicated polarized filaments, which resemble the complex structure of the interstellar gas velocities and densities. The concept of flux-tube dynamo is well known for stars (Schüssler 1993), but has never been developed for galaxies.

The Parker instability occurs in a composition of gas, magnetic field and cosmic rays placed in a gravitational field, if the magnetic field and the cosmic rays contribute to a pressure equilibrium of the system. The given pressure equilibrium of the flux tube implies that the density of the composition of gas, magnetic field and cosmic radiation is smaller than the density of the surrounding gas, which in the presence of a gravitational field leads to buoyant field lines. This situation is clearly realized in galactic halos. If the Parker instability operates, the gas together with the frozen-in magnetic field and cosmic radiation captured by the magnetic field start to ascend, forming bumps on the initially straight horizontal field lines. The portion of gas in the ascending area starts to sink along the field lines, forming the condensations of the gas in the valleys and rarefaction in summits.

Taking into account the dragging effect of turbulence in the surrounding medium we could show that the Parker instability provides a helicity of about $\alpha \sim 0.6$ km s^{-1} and that the turbulent diffusion coefficient is reduced by the effect of aerodynamic drag force, which causes an increase in dynamo efficiency. This means that a dynamo driven by Parker instability saturates faster than a classical dynamo. It also means that the magnetic field in a galaxy will always stay in the saturated state, regulated by magnetic flux loss via the Parker instability. Similar ideas for a fast dynamo were proposed by Parker (1992), who suggests a mechanism with rising and inflating magnetic lobes driven by cosmic rays.

In our first article we did not consider the effects of the cosmic rays and the underlying axisymmetric differentially rotating disc, including non-axisymmetric density waves. It is the aim of this contribution to show the results of an extended version of a flux tube dynamo, including cosmic rays in a differentially rotating disc with density waves.

The influence of the cosmic rays is obvious in face of galaxy evolution. Simply the fact that typically 90% of the gas in a galaxy has been transformed into stars means that star formation was very efficient in the early phases of evolution. For the magnetic field evolution in the flux tube model this means that the Parker instability was effectively driven by the large cosmic ray flux, since a strong star formation is always accompanied by many supernova explosions, i.e. by efficient particle acceleration. Since the cosmic ray pressure can be assumed to be dominant in star forming galaxies (see also M82 (Reuter et al. 1992)), it regulates the efficiency of the Parker instability.

The role of differentially rotating disc on the Parker instability is rather complicated. The differential forces introduce a new level of complexity to the problem. According to Foglizzo & Tagger (1994, 1995, hereafter FT'94 and FT'95) the action of differential rotation depends on the magnitude of shear but also on the radial and vertical wavenumbers of the perturbation. The differential rotation can transiently stabilize mode of long vertical wavelength, while the waves with short vertical wavelength are subject to both the Parker and the transient shearing instabilities. In the case of general 3D distribution of magnetic field the linear coupling of different modes takes place depending on the actual range of parameters including the components of the wavenumber. These results are not easily portable to the flux tube case because of the geometrical differences. Nevertheless, we confirm the close "cooperation" of the buoyancy and shearing forces and following FT'95 apply the unified name: "the Parker-shearing instability". It is however more appropriate to use the name "Parker instability" in some contexts.

The magnetic shearing (Balbus-Hawley) instability has been discussed in connection with the buoyancy and dynamo action by Brandenburg et al. (1995). The authors simulate the non linear evolution of three-dimensional magnetized Keplerian shear flow. Their system acts like dynamo that generates its own turbulence via the mentioned instabilities. They observe signatures of buoyancy as well as the tendency of magnetic field to form intermittent structures.

The plan of the paper is as follows: In Section 2 we present a general formalism for the description of the flux tube dynamics in galactic discs using the thin flux tube approximation. In Section 3 we perform a linear stability analysis and discuss the relations between the flux tube and the continuous approaches to the Parker-shearing instability. We calculate first the dynamo coefficients of the galactic flux tube dynamo for the case without shear. Then we take into account differential forces due to the galactic axisymmetric shear and the non axisymmetric density waves as well. In Section 4 we demonstrate relations between our theoretical and the recent observational results and propose a new dynamo model based on the Parker-shearing instability in galactic discs with density waves.

2. Magnetic flux tubes in galactic discs – basic equations and properties

We are going to apply the thin, slender flux tube approximation which according to Spruit (1981), Spruit and Van Ballegooijen (1982) means that the tube is assumed to be thin compared with both the scale height H of vertical density stratification and with the scale L along the tube on which the direction of its path changes. In the foregoing considerations we shall follow the formulation of Moreno-Insertis (1986) with some modifications related to the specifics of the galactic disc. We will neglect the details of the shape of the cross section of the flux tube and assume that it is circular. We will also assume that the tube is not twisted. The assumptions of the concept of the the thin, slender flux tube are extensively discussed by Schramkowski and Achterberg (1993).

2.1. Geometry of the thin flux tube

Let us describe the shape of flux tube in the 3-D volume and the cartesian reference frame rotating with the disc, by means of 3 functions

$$\begin{aligned} x &\equiv x(t,m), \\ y &\equiv y(t,m), \\ z &\equiv z(t,m) \end{aligned} \tag{1}$$

of time t and a "spacelike" parameter m – the mass measured along the tube. The lagrangian vectors

$$\boldsymbol{v} = \left(\left(\frac{\partial x}{\partial t}\right)_m, \left(\frac{\partial y}{\partial t}\right)_m, \left(\frac{\partial z}{\partial t}\right)_m \right), \tag{2}$$

$$\boldsymbol{L} = \left(\left(\frac{\partial x}{\partial m}\right)_t, \left(\frac{\partial y}{\partial m}\right)_t, \left(\frac{\partial z}{\partial m}\right)_t \right), \tag{3}$$

are respectively a velocity vector and a tangent vector. Let us specify the parameter m by the requirement that the mass flow across points $m =$ const vanishes, what means that we are going to use the lagrangian description. Having a freedom to rescale the parameter m we can chose the normalization

$$dm \equiv \xi ds, \tag{4}$$

where ξ and ds are respectively a mass per unit length and a length of an element of the flux tube. Since

$$\begin{aligned} ds^2 &\equiv dx^2 + dy^2 + dz^2 \\ &= \left(\left(\frac{\partial x}{\partial m}\right)^2 + \left(\frac{\partial y}{\partial m}\right)^2 + \left(\frac{\partial x}{\partial m}\right)^2 \right) dm^2 \end{aligned} \tag{5}$$

then

$$\mid \boldsymbol{L} \mid = \frac{1}{\xi} \tag{6}$$

The unit tangent vector $\boldsymbol{l}$ is given by

$$\boldsymbol{l} \equiv \xi \boldsymbol{L}. \tag{7}$$

Now let us define the curvature vector

$$\boldsymbol{K} \equiv \frac{\partial \boldsymbol{l}}{\partial s} \tag{8}$$

Then the curvature radius is given by

$$\frac{1}{R} \equiv K \equiv \mid \boldsymbol{K} \mid = \xi \mid \frac{\partial \boldsymbol{l}}{\partial m} \mid \tag{9}$$

and

$$\boldsymbol{n} \equiv \frac{\boldsymbol{K}}{K} \tag{10}$$

is a unit normal vector (principal normal) parallel to the curvature vector $\boldsymbol{K}$. In the following considerations we will need to decompose vectors as eg. gravitational acceleration $\boldsymbol{g}$ into components parallel and perpendicular to the unit tangent vector $\boldsymbol{l}$

$$\boldsymbol{g}_{\parallel} \equiv (\boldsymbol{g} \cdot \boldsymbol{l}) \boldsymbol{l}, \tag{11}$$

$$\boldsymbol{g}_{\perp} \equiv (\boldsymbol{l} \times \boldsymbol{g}) \times \boldsymbol{l}. \tag{12}$$

2.2. MHD equations for a thin flux tube

In order to describe the dynamics of magnetic flux tubes in a rotating reference frame of galactic discs we shall start with MHD equations in the following form

$$\frac{\partial \rho}{\partial t} + \mathrm{div}(\rho \boldsymbol{v}) = 0, \tag{13}$$

$$\rho\left(\frac{\partial \boldsymbol{v}}{\partial t} + (\boldsymbol{v}\cdot\nabla)\boldsymbol{v}\right) = \tag{14}$$

$$-\nabla p + \rho \boldsymbol{g} + \frac{1}{4\pi}\boldsymbol{j}\times\boldsymbol{B} - 2\rho\boldsymbol{\Omega}\times\boldsymbol{v} + \boldsymbol{F}_{\mathrm{diff}},$$

$$\frac{\partial \boldsymbol{B}}{\partial t} = \mathrm{rot}(\boldsymbol{v}\times\boldsymbol{B}) - \mathrm{rot}\left(\frac{1}{4\pi\sigma}\mathrm{rot}\boldsymbol{B}\right), \tag{15}$$

$$\mathrm{div}\boldsymbol{B} = 0, \tag{16}$$

where we have used traditional assignments for physical variables. The terms on the rhs. of the equation of motion (14) related to rotation need an additional explanation. The $-2\rho\boldsymbol{\Omega}\times\boldsymbol{v}$ is the Coriolis force. The additional term $\boldsymbol{F}_{\mathrm{diff}}$ is the differential force due to counteracting effects of centrifugal force and the radial component of gravitation in the shearing sheet approximation (see eg. FT'94 and references therein). The differential force will be introduced in the linearized form in the section 3. The role of the differential force due to the galactic dynamics is discussed in more details by FT'94. In addition to the above system of MHD equations we should specify additional relations which are typical for the galactic disc. Our intention is to define a general setup for the Parker-shearing instability of magnetic flux tubes which is as close as possible to the traditional continuous 3D distribution of galactic magnetic fields discussed recently in FT'94 and FT'95. This will allow us to show that the flux tube stability properties are physically very similar to stability properties of the mentioned continuous distribution of interstellar magnetic fields.

Following Parker (1966, 1967a,b) we shall assume the following isothermal equation of state for interstellar gas

$$p_g = u^2\rho, \tag{17}$$

with the sound speed of gas u independent of height in the galactic disc.

The magnetic field and cosmic ray pressures in the unperturbed state are traditionally assumed to be proportional to the gas pressure

$$p_{mag} \equiv \alpha p_g, \quad p_{cr} \equiv \beta p_g, \tag{18}$$

where α and β are constants order of 1.

The vertical equilibrium of the composition of gas, magnetic field and cosmic rays in the vertical gravitational field $\boldsymbol{g} = -\mathrm{sign(z)}|g|\boldsymbol{e}_z$ is described by the equation

$$\frac{d}{dz}\left(p_g + p_{mag} + p_{cr}\right) = \rho(z) g_z \tag{19}$$

If we assume for simplicity that g is a constant, then

$$\rho_e(z) = \rho_e(0)\exp\left(-\frac{|z|}{H}\right), \tag{20}$$

where H is the scale height of the disc given by Parker (1966)

$$H = (1+\alpha+\beta)\frac{u^2}{|g|}. \tag{21}$$

In the following we shall define our model of galactic flux tubes, which is in fact slightly different with respect to that proposed in HL'93. The present model assumes that the flux tubes

1. are composed of magnetic field, ionized gas and cosmic rays,
2. can execute motions which are almost independent on the ambient flux tubes (eg. a particular flux tube can rise due to the Parker instability, while the neighboring flux tubes are temporarily in a kind of dynamical equilibrium).
3. are distributed in space with the filling factor close to 1,
4. are initially azimuthal. This simplifying assumption will allow us to construct the equilibrium states necessary for the linear stability analysis.
5. Collisions of the flux tubes are temporarily ignored. They can lead to the magnetic reconnection processes and some reorganization of the magnetic field structure, but this topic will be discussed elsewhere.

Then, we can introduce a division between quantities specific to the flux tube interior (i) and its exterior (e). Taking into account various component of pressure we can postulate the following magneto–hydrostatic balance condition

$$p_{ig} + p_{im} + p_{icr} = p_{eg} + p_{em} + p_{ecr}, \tag{22}$$

stating that the total internal and external pressures are the same at the cylindrical flux tube boundary and the aerodynamic drag force. The aerodynamic drag force will be considered for completeness in our set of equations, however it will not be taken into account in the solutions of the present paper. We shall operate within a frame of linear stability analysis, so the aerodynamic drag force, quadratic in velocities, will be neglected. For the drag force $\boldsymbol{F}_D$ we will adopt the formula

$$\boldsymbol{F}_D \equiv -\frac{C_D\rho_e}{\pi r} \mid \boldsymbol{v}_\perp \mid \boldsymbol{v}_\perp, \tag{23}$$

where $\boldsymbol{F'}_D$ is the drag force per unit length (Schüssler 1977, Stella & Rosner 1984). C_D is a drag coefficient which, over a wide range of physical regimes characterized by subsonic motions and for Reynolds numbers lying between 30 and 10^5 (Goldstein 1938) is estimated to be $\sim 1-10$.

Now we are going to reduce the equations to the convenient form for describing the flux tube dynamics. Combining the continuity equation (13), the induction equation (15) and assuming infinite electrical conductivity one obtains

$$\frac{D}{Dt}\left(\frac{\boldsymbol{B}}{\rho}\right) = \left(\frac{\boldsymbol{B}}{\rho}\cdot\nabla\right)\boldsymbol{v} \tag{24}$$

Substituting $B \equiv \Phi/\Sigma$ and $\rho \equiv \xi/\Sigma$, where Φ is the flux across the flux tube, Σ is the cross section area, we can write

$$\frac{\boldsymbol{B}}{\rho} = \frac{\phi}{\xi}\boldsymbol{l} = \phi\boldsymbol{L}, \tag{25}$$

which leads finally to the equation

$$\frac{D\boldsymbol{L}}{Dt} = (\boldsymbol{\tau}\cdot\nabla)\boldsymbol{v} = \frac{\partial\boldsymbol{v}}{\partial m} \tag{26}$$

In the absence of Coriolis force the equation of motion (14) can be decomposed into two components: parallel and perpendicular to the tube axis

$$\left(\frac{D\boldsymbol{v}}{Dt}\right)_{\parallel} = -\frac{\xi}{\rho_i}\frac{\partial p_i}{\partial m}\boldsymbol{l} + \boldsymbol{g}_{\parallel} + \frac{\boldsymbol{F}_{diff\parallel}}{\rho_i} \tag{27}$$

$$\left(\frac{D\boldsymbol{v}}{Dt}\right)_{\perp} = \frac{B^2}{4\pi\rho_i}\boldsymbol{K} + \frac{\rho_i-\rho_e}{\rho_i}\boldsymbol{g}_{\perp} + \frac{\boldsymbol{F}_D}{\rho_i} + \frac{\boldsymbol{F}_{diff\perp}}{\rho_i}, \tag{28}$$

where $\boldsymbol{F}_{diff}$ is the differential force due to the galactic dynamics, which will be introduced in more details later on. The presence of Coriolis acceleration

$$\boldsymbol{a} \equiv -2\boldsymbol{\Omega}\times\boldsymbol{v} \tag{29}$$

couples the parallel and perpendicular components of the equation of motion.

Let us assume that the flux tubes are aligned horizontally in the initial state and assign $p_{cr}(z0) = \beta u^2\rho_e(z_0)$ to the cosmic ray pressure specific for the height z_0 in the galactic disc. Following Shu (1974) we assume that the pressure gradient of the cosmic ray gas is orthogonal to the magnetic field lines. Then, during evolution of the particular tube the internal cosmic ray pressure remains constant and equal to $p_{cr}(z0)$. Thus, we can rewrite the magneto-hydrostatic balance condition (22) as follows

$$u^2\rho_i(t,m) + \frac{B_i^2(t,m)}{8\pi} + \beta u^2\rho_e(z_0) = u^2\rho_e(z(t,m))(1+\alpha+\beta). \tag{30}$$

Due to the magnetic flux conservation we can rewrite the hydrostatic balance condition in the form

$$\rho_i = \tilde{\rho}_e - \left(\frac{\Phi}{u}\right)^2\frac{1}{8\pi\Sigma^2}, \tag{31}$$

where we denoted

$$\tilde{\rho}_e \equiv \rho_e(z)(1+\alpha+\beta) - \beta\rho_e(z_0) \tag{32}$$

and $\Phi^2 \equiv B_{i0}^2\Sigma_0^2$ with $B_{i0}^2 \equiv 8\pi\alpha u^2\rho_e(z_0)$. Since $\xi = \rho_i\Sigma$ then the equation relating the two unknowns ξ and Σ is

$$\tilde{\rho}_e\Sigma^2 - \Sigma\xi - \alpha\rho_e(z_0)\Sigma_0^2 = 0. \tag{33}$$

We find that

$$\Sigma = \frac{\xi + \sqrt{\xi^2 + 4\alpha\rho_e(z_0)\tilde{\rho}_e\Sigma_0^2}}{2\tilde{\rho}_e}. \tag{34}$$

The final form of the system of equations is as follows

$$\frac{D\boldsymbol{x}}{Dt} = \boldsymbol{v}, \tag{35}$$

$$\frac{D\boldsymbol{L}}{Dt} = \frac{\partial\boldsymbol{v}}{\partial m}, \tag{36}$$

$$\frac{D\boldsymbol{v}}{Dt} = -u^2\Sigma\frac{\partial\rho_i}{\partial m}\boldsymbol{l} + \boldsymbol{g}_{\parallel} + \frac{B^2}{4\pi\rho_i}\boldsymbol{K} + \frac{\rho_i-\rho_e}{\rho_i}\boldsymbol{g}_{\perp} - 2\boldsymbol{\Omega}\times\boldsymbol{v} + \frac{\boldsymbol{F}_D}{\rho_i} + \frac{\boldsymbol{F}_{diff}}{\rho_i}. \tag{37}$$

2.3. Basic parameters and physical units

Let us now specify the values of basic physical parameters involved in our considerations. Following Parker (1979) p. 806 we shall use parameters typical for the Milky Way as an example and take

$$g \simeq 2\cdot 10^{-9}\mathrm{cm\ s}^{-2}, \tag{38}$$

$$\rho \simeq 1.6\cdot 10^{-24}\mathrm{g\ cm}^{-3}, \tag{39}$$

which is equivalent to 1 H-atom cm^{-3}. The conventional value of the magnetic field strength is

$$B \simeq 3\cdot 10^{-6}\mathrm{G} \tag{40}$$

which leads to a magnetic pressure $p_m = B^2/8\pi = 0.4\cdot 10^{-12}\mathrm{dyn\ cm}^{-2}$. For comparison the typical value of the cosmic ray pressure is

$$p_{cr} \simeq 0.5\cdot 10^{-12}\mathrm{dyn\ cm}^{-2} \tag{41}$$

and a gas pressure

$$p_g = \rho u^2 \simeq 0.4\cdot 10^{-12}\mathrm{dyn\ cm}^{-2}, \tag{42}$$

where $u \simeq 7\mathrm{km\ s}^{-1}$ is the thermal velocity of gas. It is worthwhile to notice that Parker considers the gas pressure due to the both thermal and turbulent gas motions. Since the above estimations of gas, magnetic field and cosmic ray pressures give almost identical contributions of all the 3 components then

$$\alpha \simeq \beta \simeq 1 \tag{43}$$

and the resulting vertical scale height is

$$H \simeq 2.3 \cdot 10^2 \mathrm{pc}. \tag{44}$$

In the following considerations we shall use convenient units: 1 pc as a unit of distance and 1 Myr as a unit of time. The unit of velocity is

$$1 \text{ pc Myr}^{-1} \simeq 0.98 \text{ km s}^{-1} \tag{45}$$

and the unit of acceleration is

$$1 \text{ pc Myr}^{-2} \simeq 3.09 \cdot 10^{-14} \text{ km s}^{-2}. \tag{46}$$

In these units

$$g \simeq 0.65 \text{ pc Myr}^{-2} \tag{47}$$

and

$$\Omega \simeq 3.2 \cdot 10^{-2} \text{ Myr}^{-1}. \tag{48}$$

3. The linear stability analysis

3.1. Equations

With the aim of performing the linear stability analysis we decompose all the quantities in the 0-th and 1-st order parts. Let us start with

$$m = m_0 + m_1(m_0, t) \tag{49}$$

which leads to

$$\frac{\partial}{\partial m} = \left(1 - \frac{\partial m_1(m_0,t)}{\partial m_0}\right)\frac{\partial}{\partial m_0}. \tag{50}$$

For the flux tube which is extended along the x-coordinate in the unperturbed state, the coordinates of a given flux tube element in the linear approximation are

$$\begin{aligned} x &= \frac{m_0}{\xi_0} + x_1 && (51)\\ y &= y_1, && (52)\\ z &= z_1. && (53) \end{aligned}$$

The components of the tangent vector in the linear approximation are

$$\begin{aligned} L_{x0} &= \frac{1}{\xi_0}\left(1 - \frac{\partial m_1}{\partial m_0}\right) + \frac{\partial x_1}{\partial m_0}, && (54)\\ L_{y_0} &= \frac{\partial y_1}{\partial m_0}, && (55)\\ L_{z_0} &= \frac{\partial z_1}{\partial m_0}. && (56) \end{aligned}$$

The modulus of the tangent vector, the unit tangent vector and the curvature vector are respectively

$$\begin{aligned} \mid \boldsymbol{L} \mid &= \frac{1}{\xi_0}\left(1 - \frac{\partial m_1}{\partial m_0} + \xi_0 \frac{\partial x_1}{\partial m_0}\right), && (57)\\ \boldsymbol{l} &= \left[1, \xi_0 \frac{\partial y_1}{\partial m_0}, \xi_0 \frac{\partial z_1}{\partial m_0}\right], && (58)\\ \boldsymbol{K} &= \xi_0^2 \left[0, \frac{\partial^2 y_1}{\partial {m_0}^2}, \frac{\partial^2 z_1}{\partial {m_0}^2}\right]. && (59) \end{aligned}$$

Using the equation (36), one can find that:

$$\frac{\partial}{\partial t}\frac{\partial m_1}{\partial m_0} = 0, \tag{60}$$

which implies that

$$m_1 \equiv 0. \tag{61}$$

The mass per unit length of the tube in the linear approximation is

$$\xi = \xi_0 \left(1 - \xi_0 \frac{\partial x_1}{\partial m_0}\right). \tag{62}$$

Now we calculate ρ_{i1} in the following sequence

$$\xi_1 = -\xi_0^2 \frac{\partial x_1}{\partial m_0}, \tag{63}$$

$$\tilde{\rho}_{e1} = -\rho_e(z_0)\frac{|g|}{u^2} z_1, \tag{64}$$

$$\Sigma_1 = \frac{\Sigma_0}{2\alpha + 1}\left(\frac{\xi_1}{\xi_0} + \frac{|g|}{u^2} z_1\right), \tag{65}$$

$$\rho_{i1} = \frac{2\alpha}{2\alpha+1}\frac{\xi_1}{\Sigma_0} - \frac{1}{2\alpha+1}\frac{\xi_0}{\Sigma_0}\frac{|g|}{u^2} z_1 \tag{66}$$

Let us derive some coefficients appearing in the equation of motion (37)

$$\left(\frac{\rho_i - \rho_e}{\rho_i}\right)_1 = \left(\frac{-1}{2\alpha+1}\frac{|g|}{u^2} - \frac{1}{H}\right) z_1 + \frac{2\alpha}{2\alpha+1}\frac{\xi_1}{\xi_0}, \tag{67}$$

$$\left(\frac{B^2}{4\pi\rho_i}\boldsymbol{K}\right)_1 = v_A^2 \boldsymbol{K}_1, \tag{68}$$

where $v_A^2 = 2\alpha u^2$. The equation of tube motion (37) after linearization is

$$\begin{aligned} \frac{\partial \boldsymbol{v}_1}{\partial t} =& \frac{v_A^2}{1+2\alpha}\left(\frac{\partial^2 x_1}{\partial s^2} - \frac{(1+\alpha+\beta)}{H}\frac{\partial z_1}{\partial s}\right)\boldsymbol{l}_0 \\ &+ \frac{1+\alpha+\beta}{1+2\alpha}\left(\frac{v_A^2}{H}\frac{\partial x_1}{\partial s} - (\alpha - \beta)\frac{u^2}{H} z_1\right)\boldsymbol{g} \\ &+ v_A^2 \boldsymbol{K}_1 - 2\boldsymbol{\Omega} \times \boldsymbol{v}_1 + \boldsymbol{a}_{diff}, \end{aligned} \tag{69}$$

where s is the length parameter of the tube defined by (4) and

$$\begin{aligned} \boldsymbol{g} &= [0, 0, g], && (70)\\ \boldsymbol{l}_0 &= [1, 0, 0], && (71)\\ \boldsymbol{K}_1 &= \left[0, \frac{\partial^2 y_1}{\partial s^2}, \frac{\partial^2 z_1}{\partial s^2}\right], && (72)\\ -2\boldsymbol{\Omega} \times \boldsymbol{v}_1 &= \left[2\Omega\frac{\partial y_1}{\partial t}, -2\Omega\frac{\partial x_1}{\partial t}, 0\right] && (73) \end{aligned}$$

The linear effect of an axisymmetric differential rotation can be incorporated in a way similar to FT'94. The differential force is radial in direction and is proportional to the radial displacement in the shearing sheet approximation. There is an obvious difference between the 3D continuous case and the flux tube approach. In the continuous case the differential rotation influences also the radial wavenumber which varies linearly as a function of time (FT'94). In the flux tube approach the wavevector of the perturbation is always parallel to the tangent vector and this effect is absent since we consider (until now) only azimuthal flux tubes which are initially localized radially and vertically.

The acceleration operating on an element of the flux tube in the shearing sheet approximation is

$$\boldsymbol{a}_{diff} \equiv -4A\Omega y_1 \boldsymbol{e}_y \tag{74}$$

where

$$A = \frac{R_0}{2}\frac{d\Omega}{dR} \tag{75}$$

is the Oort constant ($A/\Omega = -1/2$ for flat rotation and $-3/4$ for the Keplerian rotation).

3.2. *The linear solution*

In a case of vanishing rotation and shear we assume the harmonic perturbation on a magnetic flux tube placed in the coordinate system (x, z) in the form

$$\begin{bmatrix} x_1 \\ z_1 \end{bmatrix} = \begin{bmatrix} X_1 \\ Z_1 \end{bmatrix} \exp i(ks - \omega t) + \text{c.c.} \tag{76}$$

where s is a length parameter measuring position along the flux tube, k is the wavenumber, x and z are the azimuthal and vertical coordinates respectively. The linearized equations describing evolution of harmonic perturbations on the flux tube lead to the linear dispersion relation

$$\det\begin{bmatrix} \frac{v_A^2 k^2}{1+2\alpha} - \omega^2 & \frac{1+\alpha+\beta}{1+2\alpha}\frac{v_A^2}{H} ik \\ \frac{1+\alpha+\beta}{1+2\alpha}\frac{v_A^2}{H}(-ik) & \frac{(\alpha-\beta)(1+\alpha+\beta)}{1+2\alpha}\frac{u^2}{H^2} + v_A^2 k^2 - \omega^2 \end{bmatrix} = 0, \tag{77}$$

where u and v_A are the thermal and Alfven speed respectively, and $H = (1+\alpha+\beta)u^2/ \mid g \mid$ is the vertical scaleheight. After the substitution of the dimensionless: azimuthal wavenumber $\bar{k} = kH$ and complex frequency $\tilde{\omega} = \omega H/v_A$, the above dispersion relation reduces exactly to the form (A1) in FT'94, which represents a case of continuous 3D distribution of magnetic field with vanishing vertical wavenumber $k_z = 0$ and the radial wavenumber $k_r = \infty$. This means that our flux tube approach is analogous to the above limiting case of continuous distribution of magnetic field.

Nevertheless, as soon as we take into account rotation (see below), the analogy becomes less clear. Our dispersion relation becomes of third order in ω^2, and the marginal stability point k_{marg} (which can be determined after the substitution of $\omega = 0$ to the dispersion relation) is the same as for no rotation. In the continuous case of FT'94, the marginal instability point is the same as for no rotation (k_P) for the radial wavenumber $k_r \to \infty$, and is smaller ($k_Q < k_P$) for $k_r = 0$. But in the limit $k_r \to \infty$, the dispersion relation of FT'94 is independent of the rotation ($\Delta(\omega^2) = 0$), and of second order in ω^2 (their eq. A1). The main difference with our approach is that the optimal wavenumber k leading to the maximum growth rate is independent of the rotation in the continuous case, whereas it depends on the rotation in the flux tube approach according to our Fig. 1. This is mathematically different, but physically acceptable, since the trends observed in our Fig. 1 and in Fig. 1. of FT'94 are very similar. Thus, we can conclude that the slender flux tube model, in addition to its observational justification, has the advantage to reduce the fully three-dimensional MHD equations to a curvilinear one-dimensional formalism. Similar conclusion has been already made by Schramkowski and Torkelson (1996) in the context of accretion discs.

In the presence of nonvanishing galactic rotation one should take into account also the radial coordinate y. In this case the linear harmonic perturbations are assumed to be

$$\begin{bmatrix} x_1 \\ y_1 \\ z_1 \end{bmatrix} \equiv \begin{bmatrix} X_1 \\ Y_1 \\ Z_1 \end{bmatrix} \exp i(ks - \omega t) + \text{c.c.} \tag{78}$$

We can write the dispersion relation in the form

$$\det\begin{bmatrix} \frac{v_A^2 k^2}{1+2\alpha} - \omega^2 & 2i\Omega\omega & \frac{1+\alpha+\beta}{1+2\alpha}\frac{v_A^2}{H} ik \\ -2i\Omega\omega & v_A^2 k^2 + 4A\Omega - \omega^2 & 0 \\ \frac{1+\alpha+\beta}{1+2\alpha}\frac{v_A^2}{H}(-ik) & 0 & \frac{(\alpha-\beta)(1+\alpha+\beta)}{1+2\alpha}\frac{u^2}{H^2} + v_A^2 k^2 - \omega^2 \end{bmatrix} = 0 \tag{79}$$

If ω is a solution of the above equation representing the Parker mode for given k, then eigenvectors are given by the following relations between constants X_1, Y_1 and Z_1

$$\frac{X_1}{Z_1} = \frac{\frac{(\alpha-\beta)(1+\alpha+\beta)}{1+2\alpha}\frac{u^2}{H^2} + v_A^2 k^2 - \omega^2}{\frac{1+\alpha+\beta}{1+2\alpha}\frac{v_A^2}{H}(ik)} \tag{80}$$

$$\frac{Y_1}{Z_1} = \frac{2i\Omega\omega}{v_A^2 k^2 + 4A\Omega - \omega^2}\frac{X_1}{Z_1} \tag{81}$$

In the Lagrangian description, the dynamo coefficients α_d and η_d can be calculated using the method applied by Ferriz-Mass et. al (1994). The expression for α_d is

$$\alpha_d \equiv \frac{\langle \boldsymbol{v} \times \boldsymbol{b} \rangle_x}{\langle \boldsymbol{B} \rangle_x} = \langle \dot{\boldsymbol{r}} \times \acute{\boldsymbol{r}} \rangle_x, \tag{82}$$

where $\boldsymbol{b}$ is the first order perturbation of magnetic field, $\boldsymbol{v} = \dot{\boldsymbol{r}}$ is the velocity of a lagrangian element of the flux tube and $\acute{\boldsymbol{r}} = \partial \boldsymbol{r}/\partial s$ is the tangent vector. The angle braces $\langle \cdots \rangle$ stand for space averaging, which in our case is related to integration over the parameter s. Similarly, the expression for diffusivity is

$$\eta_d \equiv \langle \dot{\boldsymbol{r}} \cdot \boldsymbol{r} \rangle. \tag{83}$$

Assuming only vertical diffusion for simplicity we get

$$\eta_d = \langle \dot{r}_z r_z \rangle. \tag{84}$$

This simplification is valid if horizontal displacements of the flux tube are smaller than the vertical ones. We shall indicate a case which does not fulfill this requirement.

After substitution of the linear solution one obtains

$$\alpha_d \;=\; \omega_i k Z_1(t)^2 \mathrm{Im}\left(\frac{\mathrm{Y}_1}{\mathrm{Z}_1}\right) \tag{85}$$

$$\eta_d \;=\; \frac{\omega_i}{2} Z_1(t)^2 \tag{86}$$

where $Z_1(t) = Z_1 \exp(\omega_i t)$ is the amplitude of vertical displacement of the flux tube. The neglected horizontal diffusivity $\eta_{dh} = \frac{\omega_i}{2} Y_1(t)^2$ can be easily estimated basing on vertical diffusivity since $\eta_{dh} = \eta_{dv} |Y_1/Z_1|^2$.

The magnetic Reynolds numbers and the dynamo number are defined as

$$R_\alpha \;\equiv\; \frac{\alpha_d H}{\eta_d} \tag{87}$$

$$R_\omega \;\equiv\; \frac{\Omega H^2}{\eta_d} \tag{88}$$

$$D \;\equiv\; R_\alpha R_\omega \tag{89}$$

The coefficients given by the relations (85)–(89) depend on all the involved parameters, especially on the vertical density gradient and the magnitude of shear implicitly, via the solutions of the dispersion relation (79), $\omega = \omega(k)$ and the relations (80) and (81) between components of the eigenvectors. The most relevant quantities contributing to α_d and η_d will be presented in a series of forthcoming figures.

3.3. The numerical results

Fig. 1 shows the growth rate vs. wavenumber for $\alpha = \beta = 1$, and other parameters are described in the subsection 2.3. The full line is for the case without rotation, the dotted line is for the rotation $\Omega = \Omega_G = 10^{-15}\mathrm{s}^{-1} = 0.03\mathrm{Myr}^{-1}$, the dashed line is for $\Omega = 2\Omega_G$, and dashed-dotted line is for $\Omega = 3\Omega_G$. As is well known, increasing the rotation frequency Ω dimishes the growth rate.

It is worth noting, however that the ratio of amplitudes Y_1/Z_1 of radial to vertical displacements which measures the magnitude of cyclonic deformation of the flux tube increases with rotation Ω (see Fig. 2, where dotted, dashed and dotted-dashed curves represent the same values of Ω as in Fig. 1). This ratio contributes to the α_d coefficient in (85). In addition, in the limit of $k \to 0$, $Y_1/Z_1 \to 1$ for all values of the rotation frequency.

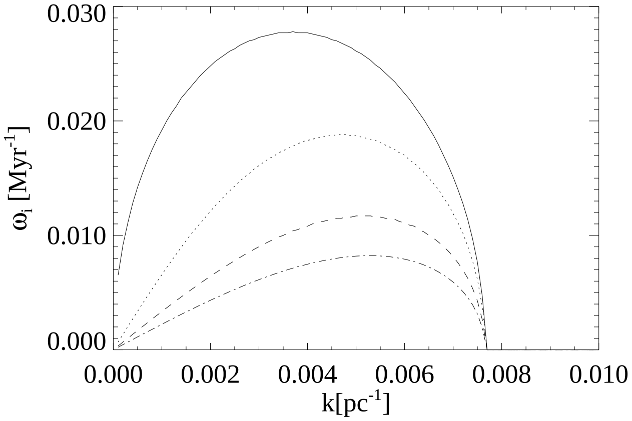

Fig. 1. The dependence of growth rate ω_i on wavenumber k for different values of the galactic rotation frequency Ω

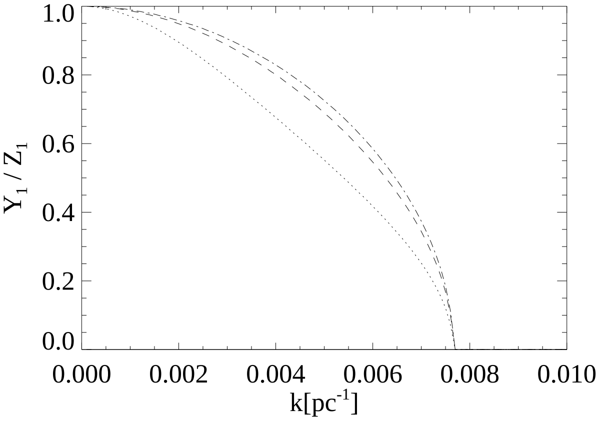

Fig. 2. The dependence of the ratio of amplitudes Y_1/Z_1 on k for the same values of values of Ω as in Fig. 1.

The dependence of α_d on k is shown in Fig. 3 for $\Omega = \Omega_G/2$ (continuous line), $\Omega = \Omega_G$ (dotted line), $\Omega = 2\Omega_G$ (dashed line) and $\Omega = 3\Omega_G$ (dashed-dotted line). The α_d coefficient is computed with the assumption that the uppermost part of the tube has passed the vertical distance equal to the vertical scale height H: $Z(t) = H$ for each value of k (for $\alpha = \beta = 1$, $u = 7$ km s^{-1} and $\mid g \mid = 2 \cdot 10^{-9}$ cm s^{-1} $= 0.65$ pc Myr^{-2} we have $H = 226$ pc). This calculation of α_d following Ferriz-Mas et al. (1994) is intended only to give a first insight about the dependence of α_d on k and Ω. It hides, however our ignorance about: (1) the initial amplitude of perturbations and (2) the final state reached by a single flux tube. Thus, within the linear theory we are not able to average over a statistical ensemble of flux tubes. Fig. 3 shows that the observed value of the galactic rotation in the solar neighborhood approximately maximizes the magnitude of the α_d

coefficient. This property could be quite important since many qualitative approaches adopt α_d proportional to Ω (see eg. Ruzmaikin et al. 1988). What we observe in our model is in contradiction with this rule.

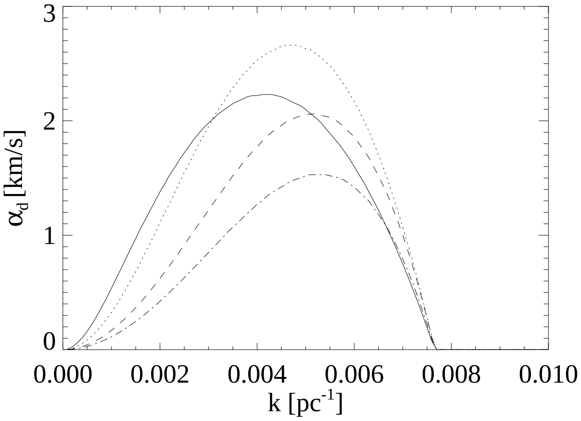

Fig. 3. The dependence of the dynamo-α_d coefficient on k for a fixed vertical displacement $Z_1 = H$ and $\Omega = 1/2, 1, 2, 3 \cdot \Omega_G$.

It is worthwhile to notice that the sign of α_d is positive for positive z coordinate, as it follows from the nature of Coriolis force which tends to slow down the rotation of rising and expanding volumes. The flow of gas directed outward of the top of the rising flux tube can be recognized as expanding in the direction along the magnetic field lines.

This feature of our model is in contrast with the results of Brandenburg et al. (1995). Strictly speaking they discuss two quantities: the mean helicity $< v \cdot \mathrm{rot} v >$ and the α_{dyn} defined as a coefficient relating the azimuthal component of electromotive force with the azimuthal mean magnetic field. While the first quantity has a proper sign ('-' in their convention of assignments, which is consistent with the positive sign of our α_d), the negative sign α_{dyn} coefficient seems to be in conflict with the positive sign of helicity.

We explain that the α_d coefficient in our model is an equivalent of the helicity $< v \cdot \mathrm{rot} v >$ used by Brandenburg et al. (1995). On the other hand we are dealing with a simple model in which the dynamo properties are derived from the dynamics of a single flux tube. Studies of the dynamics of an ensemble of flux tubes would help to find a reason of the discrepancy. Moreover, we remain in the linear regime in the present paper, thus a more detailed comparison is rather difficult.

Let us now examine the temporal evolution of the dynamo coefficients α_d, η_d, R_α, R_ω and D computed within the linear model. The results for $\alpha = \beta = 1$, $\Omega = \Omega_G$ and the maximally unstable Parker mode with $\lambda = 1330$pc are shown in Fig. 4.

It is apparent from Fig. 4 that starting from a reasonable value of the amplitude of initial perturbation ($Z_{init} = 10$pc) the α_d coefficient reaches the value of 10 km s^{-1} within the galactic rotation period $T_G = \pi/\Omega_G \simeq 200$Myr. In the same time η_d reaches the value of 1000 pc^2 Myr^{-1} $= 3 \cdot 10^{26}$ cm^2 s^{-1}. The two curves have the same slope because of the same time-dependent factor $\exp(2\omega_i t)$. For the same reason the coefficient R_α is a constant approximately equal to 1. The coefficients R_ω and D diminish with time due to growing η_d starting from the values of thousands and finishing on 1 after the time T_G. It is worth noting that we deal with an interesting situation of growing of α_d and simultaneously decreasing D.

In the case of an ensemble of flux tubes, which represents a more realistic situation, the dynamo transport coefficients will result from averaging of single flux tube contributions. Any estimations of their mean values has to be dependent on additional assumptions about a global flux tube network model. We can notice a variety of a possibilities. The feature, which seems to be the most decisive for the transport coefficients is the level of coherency of the flux tube motions. We can say that a high degree of coherency (at least in some finite size domains) should favour higher values of the mean transport coefficients, making them more comparable to the single flux tube values. In the case of low degree of coherency the system contains flux tubes more and less advanced in their buoyant rise, so their ensemble averages will represent some rather moderate values. In addition, the lower degree of coherency of flux tube motions should result in more frequent collisions between flux tubes, which in turn should limit the transport effects. Our intuition is however limited to the cases of free flux tube motions, so it is quite difficult to derive any save conclusions at the moment.

Fig. 3 gives the impression that the maximum of α_d is related to the maximum of instability of the Parker mode. It is not true in general for an arbitrary position in the (α, β)-plane, because ω_i is not the only factor in eq. (85). In order to demonstrate this effect, we fix the cosmic ray pressure putting $\beta = 1$, and vary α. The results are shown in Fig. 5.

Let us first look at the left column of graphs which shows the growth rate for various values of α and $\beta = 1$. We notice that :

1. For α comparable to 1 and larger the marginal stability point ($\omega_i = 0$) is placed near the wavelength $\lambda = 1000$ pc and the maximum instability is attained for a bit longer wavelength (eg. $\lambda(\omega_{max}) = 1330$ pc for $\alpha = 1$).
2. Decreasing α below approximately 0.6 results in a change of qualitative character of the curve $\omega_i(\lambda)$: the curve has no longer a maximum at a finite wavelength and grows monotonically with growing wavelength. For wavelengths long with respect to the marginal wave-

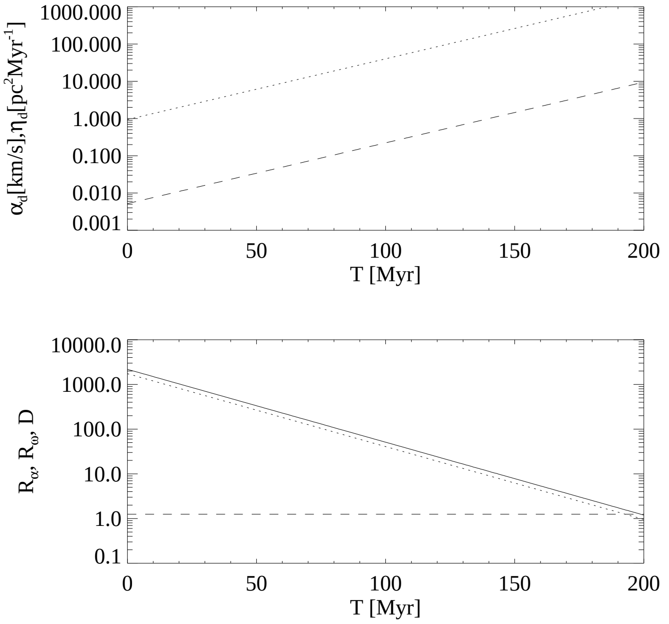

Fig. 4. The dependence of coefficients α_d (dashed line) and η_d (dotted line) on time in the linear approximation starting from an arbitrarily assumed initial vertical displacement $Z_{init} = 10$pc is shown in the upper panel. The associated dynamo numbers R_α (dashed line), R_ω (dotted line) and D (continuous line) are shown in the lower panel.

length the growth rate tends asymptotically to a constant value.

3. The marginal stability point shifts to shorter and shorter wavelengths and the maximum value of the growth rate grows while decreasing α. This can be simply explained since the magnetic tension counteracting the buoyancy force is smaller for smaller α. For a small value of $\alpha = 0.001$ (the first row) the marginal stability point is placed at a few tens of parsecs.

On the base of these remarks we find the maximum growth rate over a full range of wavelengths and fixed α, β and assign it $\omega_{i\,max}$. Next, with this growth rate we calculate the growth time $T_H(Z_{init})$ which is defined as the time which is necessary to magnify the Parker mode from given amplitude of vertical displacement $Z_{init} = 10$pc to a value $Z_1 = H$, the scale height of the Parker instability.

$$T_H(Z_{init}) = \frac{1}{\omega_{i\,max}} \log\left(\frac{H}{Z_{init}}\right) \tag{90}$$

The value of $T_H(Z_{init})$ is indicated above each row. Now let us point our attention on the second column of graphs, where α_d is computed for $T_H(Z_{init})$ as a function of λ. Note: The same value of $T_H(Z_{init})$ is used for each λ.

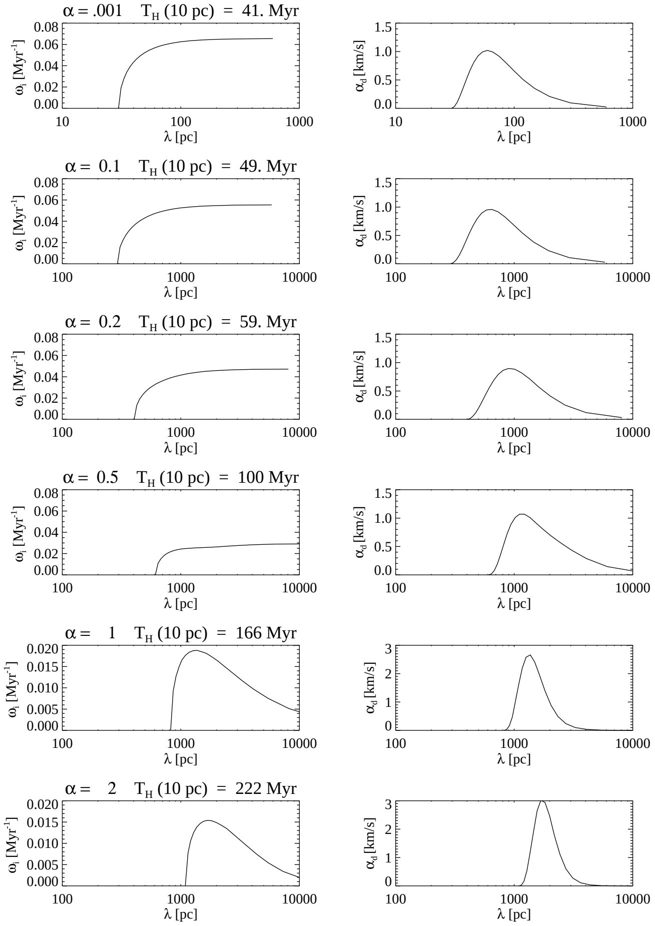

Fig. 5. The growth rate ω_i (first column) and the coefficient α_d (second column) as a function of k for $\beta = 1$ and α varying.

The result can be commented as follows: the strongest dynamo α-effect (maximum of α_d) comes from modes placed near the marginal stability point, namely the maximum of α_d is due to the modes of wavelength below 100 pc for weak magnetic fields $\alpha = 0.001$. Thus, if our flux tube is perturbed with a superposition of Parker modes which have different wavelengths and comparable initial amplitudes then we can expect a main contribution to the total α-effect due to the modes of wavelength $\lambda(\max \alpha_d)$ even if these modes do not have the maximum growth rate.

One should notice that the times $T_H(Z_{init})$ are very different depending on α and for this reason the numerical values of α_d are incomparable between rows of Fig. 5. For the sake of comparing the rate of generation of the α_d-effect as a function of α and β, it is better to fix time. Let us take $T = 50$Myr. Fig. 6. shows the values of $\mathrm{Max}(\alpha_d(\lambda))$ over the (α, β)-plane. The next Fig. 7 shows the wavelengths of the Parker modes which give rise to these maxima.

At this point we should comment on an important question which arises in relation to the above results. The question is: If we have an excess of cosmic ray pressure, wouldn't the magnetic field escape from the galaxy, in an

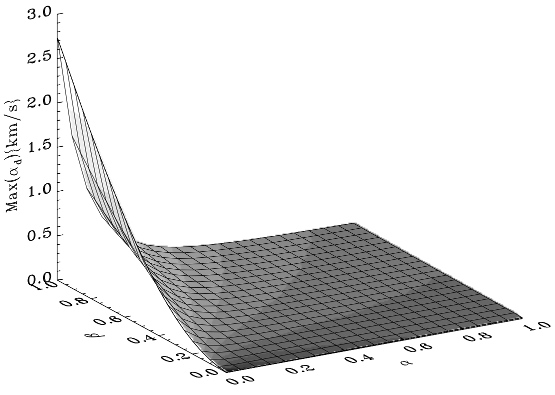

Fig. 6. The maxima of α_d as a function of α and $\beta = 1$ and α varying.

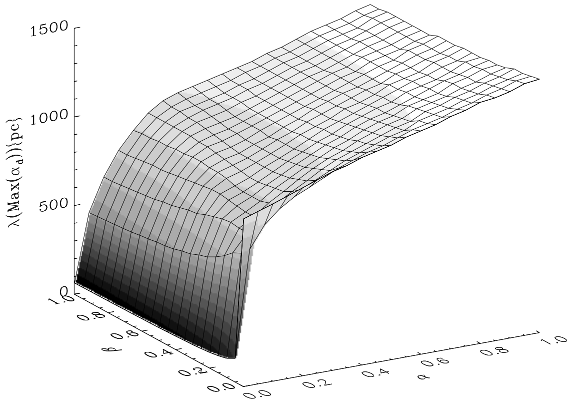

Fig. 7. The wavelengths which give rise to the maxima of α_d.

axisymmetric way, without having time to produce a dynamo ? For $\alpha = 0.001$ the dynamo coefficient α_d is maximum at $\lambda < 100pc$, but the highest growth rate is for the axisymmetric interchange mode, faster than the undulate Parker mode.

To answer this question we should note that the dominance of the axisymmetric interchange mode results from an oversimplification of the linear stability analysis. It is hard to imagine the azimuthal flux tube uniformly rising in the external medium of nonuniform density, especially in our model, in which the flux tubes are anchored at molecular clouds (HL'93, see also Beck et al. 1991). The flux tubes in between molecular clouds undergo buoyant motions, but the clouds are heavy enough to impede the long wavelength modes. In our linear stability analysis we treat the chaotic motions of clouds as a source of initial perturbations. This topic will be discussed in more details in the forthcoming paper where we perform numerical simulations of the nonlinear Parker-shearing instability of flux tubes.

Summarizing, we point out that even in the limit of very weak magnetic field strengths and high cosmic ray pressure, the dominating wavelength has to be comparable to the mean distance between clouds. This limit of is also favorable for the formation of molecular clouds via the Parker instability since the typical growth rate of the Parker instability is much higher due to the very weak magnetic tension.

This is now evident from Fig. 6. that the cosmic rays are essentially responsible for the strong α-effect in the limit of weak magnetic field (i.e. for the small α on the horizontal axis). They supply buoyancy, but in contrast to the magnetic field contribution their contribution is free of magnetic tension acting against buoyancy. This implies the enhanced growth rate as well as the fact that the marginal stability point is shifted toward the shorter wavelength. (The criterion for the Parker instability determining the marginal stability point follows from the balance between buoyancy and the magnetic tension. The magnetic tension grows with curvature of magnetic field lines proportionally to k^2.) In the result the contribution of cosmic rays is 2-folding (see the relation (85)): via the growth rate and the wavenumber as well.

3.4. The effect of an axisymmetric differential rotation

The differential force acts against the radial component of the magnetic tension which depends on the value of the wavenumber k. Let us fix our attention on the the case $\alpha = \beta = 1$, $\Omega = \Omega_G$ and all other parameters like those used in Figs. 1, 2 and 3. The solutions of the dispersion relation (79) for nonvanishing differential force together with the ratio of amplitudes Y_1/Z_1 and the α_d coefficient are presented in Fig. 8.

The results can be commented as follows:

1. The curves of growth rate are split into 2 separate parts in each case. The minimum between them is placed at the wavenumbers $k = k_{crit}$ related to the balance between: the radial component of the magnetic tension, the radial component of the Coriolis force and the differential force. The right hand parts are associated with vanishing oscillation frequencies and the left hand parts with non-vanishing ones (see the right top panel). This means that in the limit of small wavenumbers we deal with propagating waves in contrast to the stationary waves in the range between k_{crit} and k_{marg}, where k_{marg} is assigned to the usual marginal stability point. In this respect the Parker–shearing instability is in the range (k_{crit}, k_{marg}) similar to the Parker instability without shear. The typical phase speeds ω_r/k are close to the Alfven speed $v_A \sim 10$km/s.
   It would be convenient to introduce names of the right-hand and left-hand ranges. We would suggest splitting the name *Parker-shearing instability* into *the Parker*

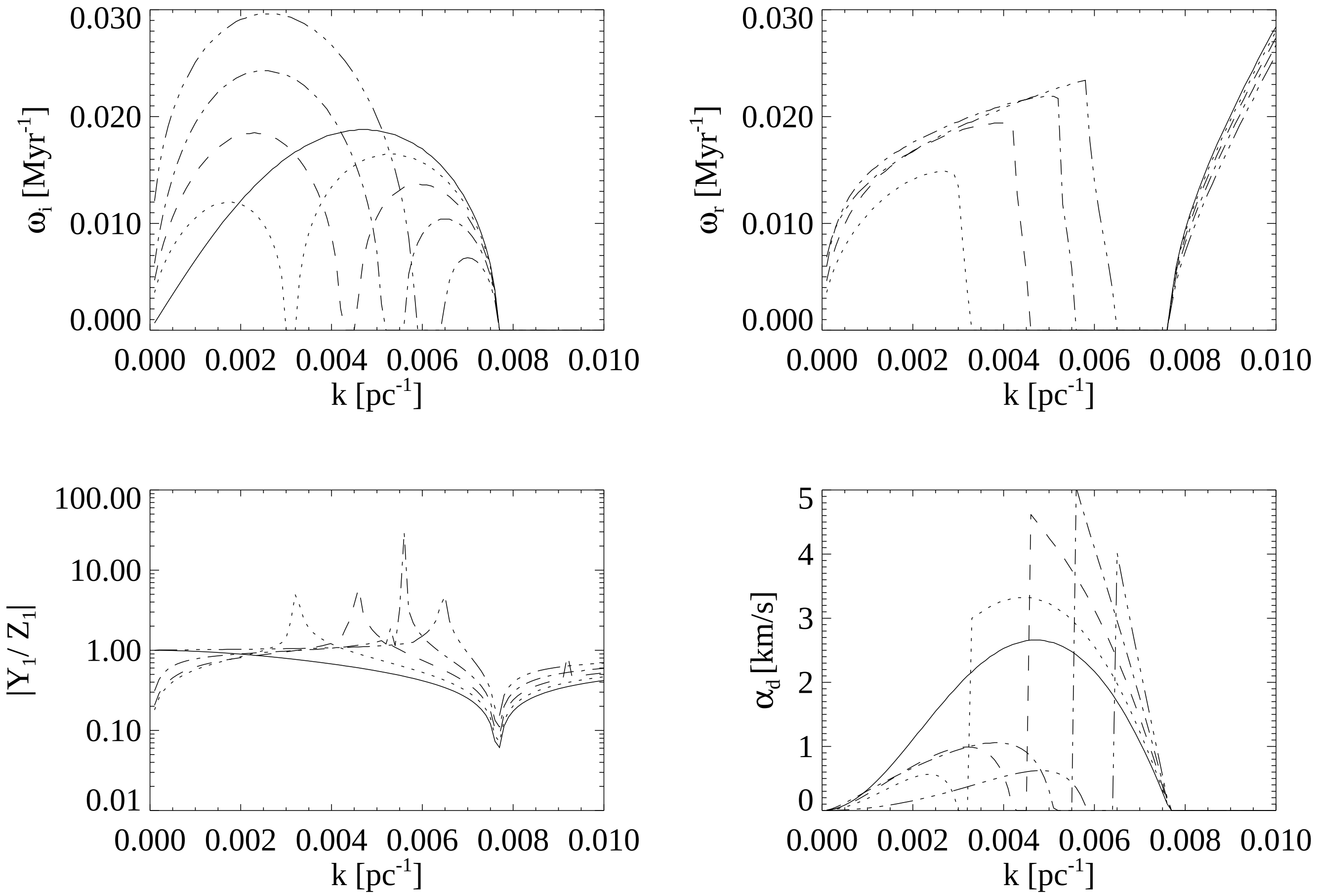

Fig. 8. The dependence of growth rate, frequency, $|Y_1/Z_1|$ amplitude ratio and α_d on wavenumber k for fixed $\Omega = \Omega_G$ and the differential force related to $A/\Omega = 0$ (full line), -1/4 (dotted line) -1/2 (dashed line), -3/4 (dot-dashed line) and -1 (3*dot-dashed line).

range for $k_{crit} < k < k_{marg}$ and *the shearing range* for $0 < k < k_{crit}$.

2. The modulus of the ratio of radial to vertical displacement amplitudes $|Y_1/Z_1|$, is strongly modified with respect to the case without shear. The reduction of the restoring radial magnetic tension by the opposite differential force results in enhanced radial (Y) excursions of the flux tube for perturbations placed near the critical wavenumber. One should notice that only the imaginary part $\mathrm{Im}(\mathrm{Y}_1/\mathrm{Z}_1)$ contributes to α_d. The $\mathrm{Im}(\mathrm{Y}_1/\mathrm{Z}_1)$ is identical to $|Y_1/Z_1|$ in the Parker range and is much smaller than $|Y_1/Z_1|$ in the shearing range because of an additional phase shift between the radial and vertical displacements. This gives rise to the apparent jump of α_d at the critical wavenumber k_{crit}. In the Parker range the α-effect is strongly magnified and in the shearing range it is strongly diminished with respect to the vanishing shear case.
3. We can expect also an enhanced horizontal diffusion near k_{crit} since the radial displacements of the flux tube are approximately ten times larger than the vertical ones. Then, the horizontal diffusivity can be even two orders of magnitude larger than the vertical diffusivity. This feature makes a big qualitative difference with respect to the superbubble model by Ferriere (1996), where the vertical diffusivity is comparable or larger to the horizontal one depending on the galactic height.

3.5. Periodic variations of differential force due to the linear density wave

Let us try to imagine what happens in the presence of density waves. Let us assume that a single wavelength of the Parker–shearing instability dominates, related to $k_0 = 0.005\mathrm{pc}^{-1}$. We expect that the density wave introduces periodic modification of the differential force around the mean value resulting from the axisymmetric rotation.

Assume that the amplitude of these oscillations is sufficiently large to cause the boundary between the Parker range and the shearing range to oscillate around k_0 depending on the phase of density wave. **Then, we can expect a switch–on and –off mechanism of the α-effect.**

Now, we shall recall some basic properties of density waves. Stellar density waves in the galactic disc introduce periodic perturbations to the axisymmetric gravitational potential $\Phi_0(R)$ (see eg. Binney & Tremaine 1987, p. 386-388). In the linear approximation and with the assumption that the density waves are tightly wound, these perturbations have the following form

$$\Phi_1(R,\varphi) = F\cos(k_{dw}R + m\varphi), \tag{91}$$

where k_{dw} is the radial wavenumber of the density wave, m is the azimuthal wavenumber of the density wave, R and φ are the radius and the azimuthal angle in galactic disc. The amplitude F can be estimated from the condition for cloud–cloud collisions (eqn. (6-75) of Binney & Tremaine 1987). Taking into account $g = 1$ for which the collisions start to occur, we can estimate

$$F \simeq \frac{\mid \kappa_0^2 - \omega_{dw}^2 \mid}{k_{dw}^2}. \tag{92}$$

If we introduce a typical value of the epicyclic frequency $\kappa_0 = 1.2\Omega_G$, and the oscillation frequency of the density wave $\omega_{dw} = 0.75\kappa_0$ and $k_{dw} = 2 \cdot 10^{-3}\mathrm{pc}^{-1}$ then

$$F = 150\frac{\mathrm{pc}^2}{\mathrm{Myr}^2} \tag{93}$$

The gravitational acceleration due to this potential is

$$a_{r1} = -\frac{\partial \Phi_1}{\partial R} = k_{dw}F\sin(k_{dw}R + m\varphi) \tag{94}$$

For our purposes it will be necessary to know the differential acceleration due to the density wave acting on 2 points displaced by ΔR in the radial direction

$$\Delta a_{r1} = \frac{\partial a_{r1}}{\partial R}\Delta R = k_{dw}^2 F\cos(k_{dw}R + m\varphi)\Delta R \tag{95}$$

The constant

$$A_{r1} \equiv k_{dw}^2 F \tag{96}$$

describes the amplitude of the oscillations of the differential force. Substituting the numerical values for k_{dw} and F we obtain

$$A_{r1} = 0.6 \cdot 10^{-3} Myr^{-2}, \tag{97}$$

while the differential acceleration resulting from axisymmetric rotation is described by the analogous constant $A_{r0} = -4A\Omega \simeq 2 \div 3 \cdot 10^{-3} Myr^{-2}$ depending on the type of the rotation curve. We notice that the 'top–bottom' amplitude of oscillations of the differential force is of the order of 50% of the mean value coming from the axisymmetric differential rotation.

It appears that the differential acceleration due to the density waves is comparable to the differential acceleration due to the axisymmetric differential rotation even if the perturbation of interstellar gas is at the limit of linear regime. This limit is related to approximately 1% magnitude of perturbation of the axisymmetric gravitational potential (Roberts, 1969; Shu et al. 1973). From the above considerations one can easily derive the relevant relation

$$\frac{A_{r1}}{A_{r0}} = \frac{\pi^2 R^2}{\lambda_{dw}^2}\frac{\Omega}{-A}\frac{\Phi_1}{\Phi_0} \tag{98}$$

where λ_{dw} is the radial wavenumber of the density wave and Φ_1/Φ_0 is the relative magnitude of the axisymmetric gravitational potential perturbation. This is obvious that typically the density wave has the wavelength much shorter than the value of the radial coordinate at a given point in the galactic disc, and then A_{r1}/A_{r0} can be be larger than Φ_1/Φ_0 even by a factor of a few tens.

This implies that the switch–on and –off mechanism of the α-effect is really possible in observed galaxies.

Let us try to figure out what is the phase difference between the oscillations of differential force and the density maxima of spiral arms. The density maxima coincide with minima of the periodic component of gravitational potential. The periodic acceleration is directed toward the density concentrations and the derivative of the periodic acceleration is in phase with the potential perturbations. This means that the density wave tends to decrease the differential force in arms and increase it in the interarm regions. As we already suggested this effect can cause that a perturbation with some dominating wavenumber k_0 moves from the Parker range to the shearing range periodically. Now, we have fixed that the Parker range coincides with arms and the shearing range with interarm regions. The validity of the current formulation of the problem depends on time available between the passages of two neighboring arms of the galactic spiral structure. One can say that our approach is valid if the growth time of the Parker instability is much shorter than the density wave oscillation period. This criterion is well fulfilled in the limit of weak magnetic field strength and high cosmic ray pressure, but it is fulfilled only marginally if the magnetic pressure is comparable to the gas pressure.

4. Conclusions

Conclusions which follow from our calculations can be splited in two groups. The first group is related mainly to the cosmological generation of the galactic magnetic fields due to the Parker instability. In this case the presence of shear magnifies the dynamo effect, however it is of secondary importance. The second group concerns the contemporary evolution of magnetic field in galaxies. Some observed features of magnetic field in nearby galaxies seem to be a signature of the active role of differential forces due to the axisymmetric shear and the density waves as well.

The first group of conclusions is as follows:

1. Contrary to the common opinion that the Parker instability was ineffective in the past we note that weak magnetic field enables a fast growth of Parker modes due to a lack of magnetic tension if only the cosmic ray pressure was high enough.
2. For weak magnetic fields the strong cosmic ray pressure cause the main contribution to the dynamo α-effect to come from waves shorter then 100 pc, which is good for the "mean field dynamo theory" since the shorter waves mean a better statistics.
3. If the magnetic field strength exceeds a few μG, the time necessary for α_d to reach 1 km/s exceeds the galactic rotation period and the discussed process can only sustain the existent magnetic field strength.

Based on these conclusions we can formulate a hypothesis that during galaxy formation stars started to form in the presence of a very weak magnetic field, producing an excess of cosmic ray pressure over the magnetic pressure. The excess of cosmic rays forced a strong dynamo action converting the exceeding cosmic ray energy to the magnetic energy. The contemporary equipartition is the result of this process.

This scenario finds its convincing proof in the observational fact that at high redshifts the number of blue objects, i.e. excessively starbursting galaxies, is much larger than today (e.g. Lilly 1993). Just recently, an analysis of the deepest available images of the sky, obtained by the Hubble Space Telescope reveals a large number of candidate high redshift galaxies, up to redshifts $z \geq 6$. The high-redshift objects are interpreted as regions of intense star formation associated with the progenitors of present-day normal galaxies, at epochs that may reach back 95% of the time to the Big Bang (Lanzetta et al. 1996).

We note that the effective action of a "Parker-dynamo" would also offer a solution for the problem of magnetization of the intergalactic medium. Especially the origin of magnetic fields in the radio halos of galaxy clusters, like the Coma-cluster is still an open question (Burns et al. 1992). Our scenario may provide the backstage for magnetizing large cosmic volumes via galactic winds. If all galaxies go through a phase of intense star formation, they will drive galactic winds, which like in the case of the standard starburster M82 will have strong winds, which transport relativistic electrons and magnetic fields into the intergalactic medium (Kronberg and Lesch 1996). The radio halo of M82 is about 10 kpc in radius with a mean field of about 10μG (Reuter et al. 1992).

The second group of conclusions is related closely to the galactic dynamics. **We predict a strong α effect in arms and very weak one between arms**. Let us recollect that the magnified α-effect in the Parker range near the critical wavenumber k_{crit} is the result of shearing forces which counteract the radial magnetic tension and enable large amplitudes of radial deformations of the azimuthal flux tube. We expect also an enhanced amount of the chaotic component of magnetic field in arms.

Then, we can propose a new galactic dynamo model relying on a cyclic process composed of the action of galactic axisymmetric differential rotation, density waves, Parker-shearing instability and magnetic reconnection. The cyclic process is as follows: The α-effect due to the Parker-shearing instability is controlled by the magnitude of shear. We postulate that the initial state of perturbation can be determined by small irregularities in the interarm region (like e.g the velocities of small molecular clouds). Then the approaching arm induces a strong α-effect due to Parker-shearing instability and in consequence the dynamo action. The magnetic field becomes irregular due to the vertical and horizontal displacements of flux tubes. As it follows from Fig. 8 the horizontal displacements exceed significantly the vertical ones. When the arm passes considered region by, the α-effect becomes suppressed again. Then the enhanced shear of interarm region makes order in horizontal structure of magnetic field and reconnection removes the vertical irregularities, thus our model predicts a more regular magnetic field in the interarm regions. We are in the state which is similar to the initial one with the difference in the strength of magnetic field which is stronger now due to the recent dynamo action. The characteristic feature of the proposed model is the dynamo action (strictly speaking the α-effect) operating exclusively in spiral arms.

These results perfectly explain observational results of Beck & Hornes (1996). The sharp peaks of the total power and the polarized emission presented in their Fig. 3 suggest that the switch–on and –off mechanism of the α-effect of our model takes place in NGC 6946.

Moreover, the mentioned observations seem to contradict the critics of the dynamo mechanism by Kulsrud and Anderson (1992). The fast uniformization of the nonuniform magnetic field in spiral arms has the observed time scale order of the fraction of galactic rotation period. This means that processes faster than the ambipolar diffusion play a role in dissipation of irregular component of the galactic magnetic field. Since our model represents a kind of the fast dynamo (Parker, 1992) we postulate that the magnetic reconnection can efficiently remove the short wavelength irregularities of flux tubes.

The application of two intrinsic instabilities of magnetized differentially rotating galactic discs leads to interesting conclusions about the "magnetic history" of the Universe. The magnetic fields in the high-redshift objects is already as strong as the magnetic fields in nearby galaxies. Thus, energetically nothing has happened for many Gigayears in disc galaxies, their magnetic energy density stays at the level of equipartition. This already indicates that global saturation mechanisms like the Parker-instability are at work in these objects. Adding observed properties of the high-redshift objects, namely intense star formation, accompanied by effective production of cosmic rays, we have developed a very promising scenario for the evolution of magnetic fields in galaxies, which is able to reproduce the magnetic structure in nearby galaxies and the saturation of magnetic energy density during galactic evolution.

Acknowledgements. It is a pleasure to thank Thierry Foglizzo for the very detailed and fruitful discussions during the work on this paper and for his critical reading of the manuscript. We thank also Marek Urbanik and an anonymous referee for their valuable comments. MH thanks the Max-Planck-Institut für Astrophysik, Garching, Germany for a kind hospitality. This work was supported by the grant from Polish Committee for Scientific Research (KBN), grant no. PB 0479/P3/94/07.

References

Beck, R., Berkhuijsen, E.M., Bajaja E., 1991, in *Dynamics of Galaxies and Molecular Cloud Distribution*, IAU Symp. 146, F. Combes, F., Casoli (eds.)
Beck, R., Hoernes, P., 1996, Nature, 379, 47
Beck, R., Brandenburg, A., Moss, D. et al., 1996, ARAA (in press)
Brandenburg, A., et al., 1995, ApJ, 446, 741
Burns, J.O., Sulkanen, M.E., Gisler, G.R., Perley, R.A., 1992 ApJ338, L49
Camenzind, M., Lesch, H., 1994, A&A, 284, 411
Goldstein, S., 1938, *Modern Developments in Fluid Dynamics* (Oxford: Claredon Press)
Ferriere, K., 1993, ApJ, 404, 162
Ferriere, K., 1996, A&A, 310, 455
Ferriz-Mass, A., Schmidt, D., Schüssler, M., 1994, A&A289, 949
Foglizzo, T., Tagger, M., 1994, A&A, 287, 297 (FT'94)
Foglizzo, T., Tagger, M., 1995, A&A, 301, 293 (FT'95)
Hanasz, M., Lesch, H., 1993, A&A, 278, 561 (HL'93)
Kaisig, M., Rüdiger, G., Yorke, H.W., 1993, A&A, 274, 757
Kronberg, P.P., 1994, Rep. Prog. Phys. 57, 325
Kulsrud, R,M., 1990, in *Physical Processes in Hot Cosmic Plasmas* W. Brinkmann, A.C. Fabian, and F. Giovanelli (eds.), Kluwer, Dordrecht, p. 247
Kulsrud, R.M., Anderson, S.W., 1992, ApJ, 396, 606
Lanzetta, K.M., Yahil, A. Fernandez-Soto, A., 1996, Nature, 381, 759
Lesch, H., Chiba, M., 1995, A&A, 297, 305
Lilly, S., 1993, in *The Environment and Evolution of Galaxies*, ed. J.M. Shull and H.A. Thronson, Kluwer, Dordrecht, p. 143
Moreno-Insertis, F., 1986, A&A, 166, 291
Moreno-Insertis, F., 1995, in *Solar and Astrophysical MHD Flows* (ed. K. Tsinganos)
Parker, E.N., 1979, *Cosmical Magnetic Fields*, Oxford
Parker, E.N., 1955, ApJ, 121, 491
Parker, E.N., 1967a, ApJ, 149, 517
Parker, E.N., 1967b, ApJ, 149, 535
Parker, E.N., 1992, ApJ, 401, 137
Reuter, H.P., Klein, U., Lesch, H. et al., 1992, A&A, 256, 10
Roberts, W.W, 1969, ApJ, 158, 123
Ruzmaikin, A.A., Shukurov, A.M., Sokoloff, D.D., 1988, *Magnetic Fields in Galaxies*, Reidel, Dordrecht
Schramkowski, G.P., Achterberg, A., 1993, A&A, 280, 313
Schramkowski, G.P., Torkelson, U., 1996, A&AR, 7, 55
Schüssler, M., 1977, A&A, 56, 439
Schüssler, M., 1993, in: *The Cosmic Dynamo* F. Krause, K.-H. Rädler, G. Ruediger (eds.), IAU-Symp. No. 157, Kluwer, Dordrecht, p. 27
Shu, F.H., 1974, A&A, 33, 55
Shu F.H., Milone, V., Roberts, W.W., 1973, ApJ, 183, 819
Spruit, H.C., 1981, A&A, 98, 155
Spruit, H.C., Van Ballegooijen, A.A., 1982, A&A, 106, 58
Stella, L., Rosner, R., 1984, ApJ, 277, 312
Wolfe, A.M., Lanzetta, K.M., Oren, A.L., 1992, ApJ, 388, 17

This article was processed by the author using Springer-Verlag LaTeX A&A style file *L-AA* version 3.